iScience

CellPress
OPEN ACCESS

Article

Antibody attributes, Fc receptor expression, gestation and maternal SARS-CoV-2 infection modulate HSV IgG placental transfer

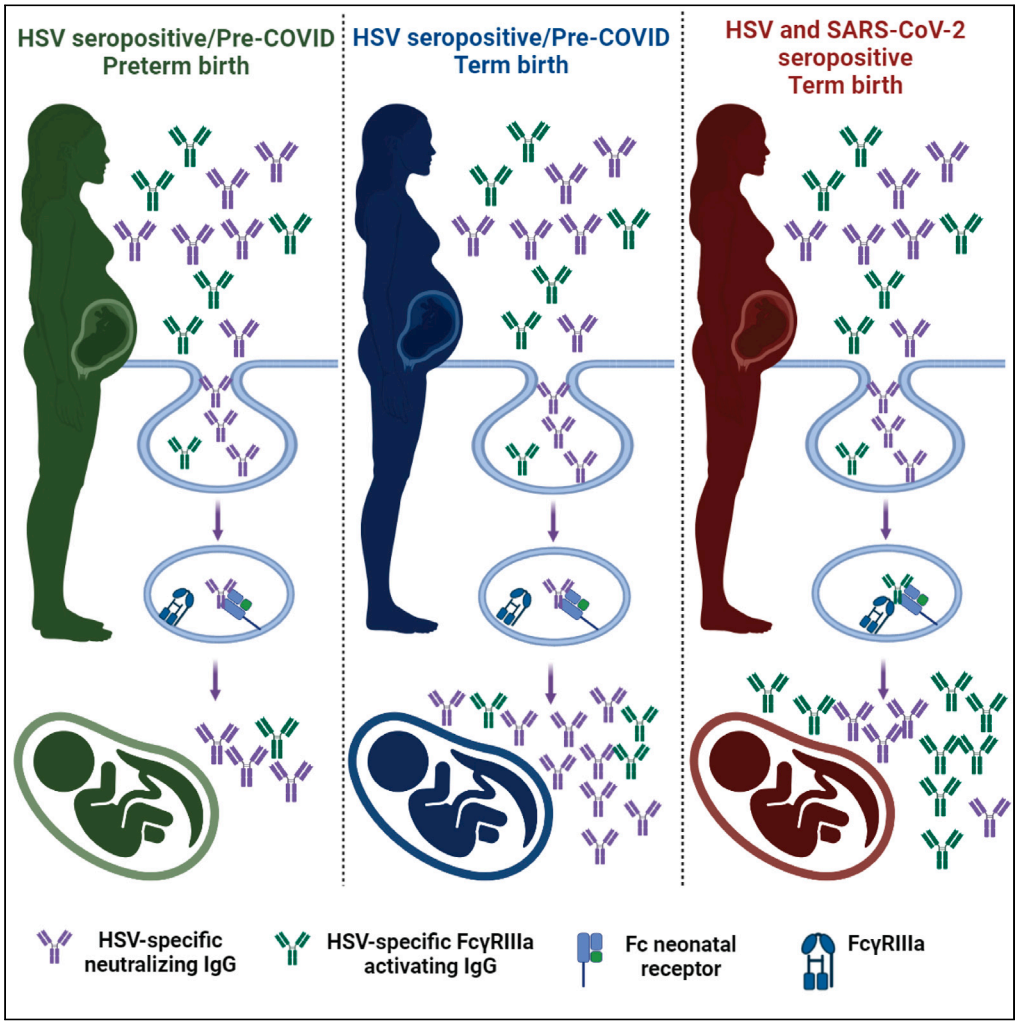

Aakash Mahant Mahant, Fatima Estrada Trejo, Jennifer T. Aguilan, Simone Sidoli, Sallie R. Permar, Betsy C. Herold

betsy.herold@einsteinmed.edu

Highlights

HSV neutralizing antibodies transfer more efficiently than ADCC-mediating IgG

Placental transfer of HSV-antibodies is reduced in preterm deliveries

Placental transfer efficiency maps to antigen target, glycans, and FcRn affinity

ADCC-mediating IgG transfer is increased with maternal SARS-CoV-2 infection

Mahant et al., iScience 26, 107648
September 15, 2023
https://doi.org/10.1016/j.isci.2023.107648

iScience

CellPress
OPEN ACCESS

Article

Antibody attributes, Fc receptor expression, gestation and maternal SARS-CoV-2 infection modulate HSV IgG placental transfer

Aakash Mahant Mahant,[1] Fatima Estrada Trejo,[1] Jennifer T. Aguilan,[1] Simone Sidoli,[1] Sallie R. Permar,[2] and Betsy C. Herold[1,3,*]

SUMMARY

Antibody-dependent cellular cytotoxicity (ADCC) is associated with protection against neonatal herpes. We hypothesized that placental transfer of ADCC-mediating herpes simplex virus (HSV) immunoglobulin G (IgG) is influenced by antigenic target, function, glycans, gestational age, and maternal severe acute respiratory syndrome coronavirus 2 (SARS-CoV-2) infection. Maternal and cord blood were collected from HSV-seropositive (HSV+) mothers pre-COVID and HSV+/SARS-CoV-2+ mothers during the pandemic. Transfer of HSV neutralizing IgG was significantly lower in preterm versus term dyads (transfer ratio [TR] 0.84 vs. 2.44) whereas the TR of ADCC-mediating IgG was <1.0 in both term and preterm pre-COVID dyads. Anti-glycoprotein D IgG, which had only neutralizing activity, and anti-glycoprotein B (gB) IgG, which displayed neutralizing and ADCC activity, exhibited different relative affinities for the neonatal Fc receptor (FcRn) and expressed different glycans. The transfer of ADCC-mediating IgG increased significantly in term SARS-CoV-2+ dyads. This was associated with greater placental colocalization of FcRn with FcγRIIIa. These findings have implications for strategies to prevent neonatal herpes.

INTRODUCTION

Active or passive immunization during pregnancy provides an important opportunity to improve maternal health and reduce neonatal morbidity and mortality from infectious diseases.[1,2] Maternal vaccination can boost the placental transfer of protective antibodies (Abs) as evidenced by studies of inactivated influenza, acellular pertussis, and, most recently, severe acute respiratory syndrome coronavirus 2 (SARS-CoV-2).[3–6] Immunizations may be most effective when administered early in the third trimester as placental syncytiotrophoblast expression of the neonatal Fc receptor (FcRn), which plays the dominant role in immunoglobulin G (IgG) transfer, increases after 28 weeks of gestation.[7] The affinity of IgG for the FcRn is influenced by IgG subclass and IgG glycans.[8–10] For example, while the A297-N-linked glycosylation site of Fc is not in the FcRn binding site, glycans at this site affect the conformation and modify the affinity for the FcRn.[11,12] IgG1 has the highest affinity followed by IgG4, IgG3, and IgG2, and sialylated and digalactosylated Fc glycans are associated with higher FcRn affinity.[7,13–15] The antigenic target of IgG also affects placental transfer, presumably because it may affect which subclass is elicited, glycan modifications, and conformation of Fc upon fragment antigen binding (Fab).

Both herpes simplex virus type 1 and type 2 (HSV-1 and HSV-2) are transmitted perinatally during clinically evident, or more commonly, clinically silent genital tract shedding.[16–19] In 2018, it was estimated that there were ~14,000 annual (4,000 HSV-1 and 10,000 HSV-2) cases of neonatal herpes, although the incidence of neonatal HSV-1, which has emerged as the more common cause of primary genital infections in the United States and other countries, is increasing.[19] Risk factors for neonatal HSV disease include primary or first-episode maternal infection in the third trimester, preterm birth, maternal age less than 21 years, and invasive monitoring, which may disrupt the protective epithelial barrier.[17,18] The increased risk for neonatal disease following primary compared to reactivating HSV may reflect higher maternal HSV viral loads as well as limited placental transfer of HSV-specific IgG.[20] The increased risk with preterm birth may also be linked to reduced transfer of HSV-specific IgG, although this has not been well studied.[21]

The function of the transferred Abs may also impact the clinical outcome. Neonates who acquired higher levels of Abs that mediate antibody-dependent cellular cytotoxicity (ADCC) from their mothers were more likely to have disease limited to the skin whereas those with low levels of ADCC-mediating Abs were more likely to have disseminated disease after controlling for the nAb titer.[22] Importantly, primary HSV infection elicits a predominantly neutralizing response with little or no ADCC detected until at least 6 months following primary infection.[23]

[1]Departments of Microbiology and Immunology, Obstetrics-Gynecology and Women's Health, and Biochemistry Albert Einstein College of Medicine, Bronx, NY 10461, USA
[2]Department of Pediatrics, Weil Cornell Medicine, New York, NY 10021, USA
[3]Lead contact
*Correspondence: betsy.herold@einsteinmed.edu
https://doi.org/10.1016/j.isci.2023.107648

Table 1. Demographic and clinical characteristics of study participants (presented as n unless otherwise indicated)

Variable	pre-COVID (n = 41)		SARS-CoV-2+ (n = 36)		
	Term (A) (n = 25)	Preterm (B) (N = 16)	Term (C) (n = 28)	Preterm (D) (n = 8)	p value ANOVA (Dunn's multiple comparisons test)
Maternal Age (years) (Median [IQR])	28 [25–35]	31 [26–34]	28 [24–33]	25 [23–33]	NS
Ethnicity: Hispanic: Non-Hispanic	16:9	9:7	23:5	6:2	NS (chi-square)
Race: Black: White: Asian: Other	12:3:1:9	9:2:0:5	18:1:2:7	3:2:2:1	NS
HSV serostatus HSV-1$^+$: HSV-2$^+$: Dual+	17:4:4	14:1:1	22:4:6	8:0:0	NS (chi-square)
Neonatal gestational age (weeks) (median [IQR])	39 [38–40]	32 [30–34]	39 [37–40]	33 [32–34]	0.0001 A vs. B $p < 0.0001$ C vs. D $p < 0.001$
Delivery route Vaginal: C-Section	14:11	10:6	21:7	6:2	NS (chi-square)
Neonatal Sex Male: Female	13:12	10:6	15:13	4:4	NS (chi-square)
Days from maternal blood collection to delivery (Median [range])	55 [0–79]	0 [0–18]	0 [0]	0 [0]	0.001 A vs. B $p < 0.0001$
Pregnancy complications Chorioamnionitis Preeclampsia	0 1 (4.0%)	1 (6.2%) 4 (25%)	0 0	0 0	NS (chi-square) $p < 0.01$
Days from SARS-CoV-2 PCR + test to delivery (Median [range])			2 [0–128]	1 [0–56]	NS
COVID-19 Severity None: Mild: Moderate: Severe			17:8:3:0	1:3:2:2	$p < 0.05$ (chi-square)

NS = non-significant ($p > 0.05$).

Maternal coinfections also may modulate placental transfer of pathogen-specific IgG by several mechanisms including an increase in total maternal IgG levels and subsequent competition for FcRn, placental inflammation, and changes in placental expression of FcRn and FcγRIIIa, the receptor associated with ADCC responses.[24,25] For example, maternal malaria infection is associated with decreased transport of measles but not tetanus Abs, whereas maternal HIV is associated with decreased placental transfer of both measles and tetanus Abs.[13,26,27] In contrast, the transfer of influenza- and pertussis-specific Abs were preserved in pregnant women infected with SARS-CoV-2 during the third trimester.[25]

While early recognition and treatment with acyclovir have reduced the mortality of neonatal HSV disease, morbidity remains high. Thus, there is an urgent need to develop safe and effective vaccines and/or monoclonal Abs to prevent maternal infection, boost maternal antibody titers and subsequent placental transfer, and/or treat infected neonates. There is little data on the determinants of placental transfer of HSV-specific IgG. The current study, therefore, was designed to compare the quantity, function (neutralization, complement component C1q binding, or FcγRIIIa activation as a biomarker of ADCC[21,28–32]), and antigenic targets of HSV-specific IgG in mother-cord blood dyads who delivered at term compared to preterm and to evaluate whether maternal SARS-CoV-2 coinfection during pregnancy impacted the transfer by comparing maternal HSV-seropositive (HSV+) pre-COVID and maternal HSV+SARS-CoV-2-coinfected (HSV+/SARS-CoV-2+) dyads.

RESULTS

Demographics and clinical characteristics of study participants

Maternal and cord blood were obtained from HSV+ mothers and their newborns who delivered between October 2018 and December 2019 (pre-COVID, n = 41) and HSV+/SARS-CoV-2+ mothers (defined by a positive maternal SARS-CoV-2-specific nasopharyngeal PCR test at enrollment) and newborns who delivered between April and December 2020 (n = 36) (Table 1). To evaluate the impact of preterm delivery on placental transfer of IgG, both groups were dichotomized at 37 weeks of gestation into term and preterm cohorts. There were no significant differences in maternal demographics, although more pre-COVID preterm mothers had preeclampsia ($p < 0.01$, chi-square). In addition, maternal blood was obtained earlier relative to delivery in the pre-COVID term compared to the other groups ($p < 0.001$, Kruskal-Wallis with Dunn's multiple comparison test) and therefore this variable was included in linear regression models as further described in the following.

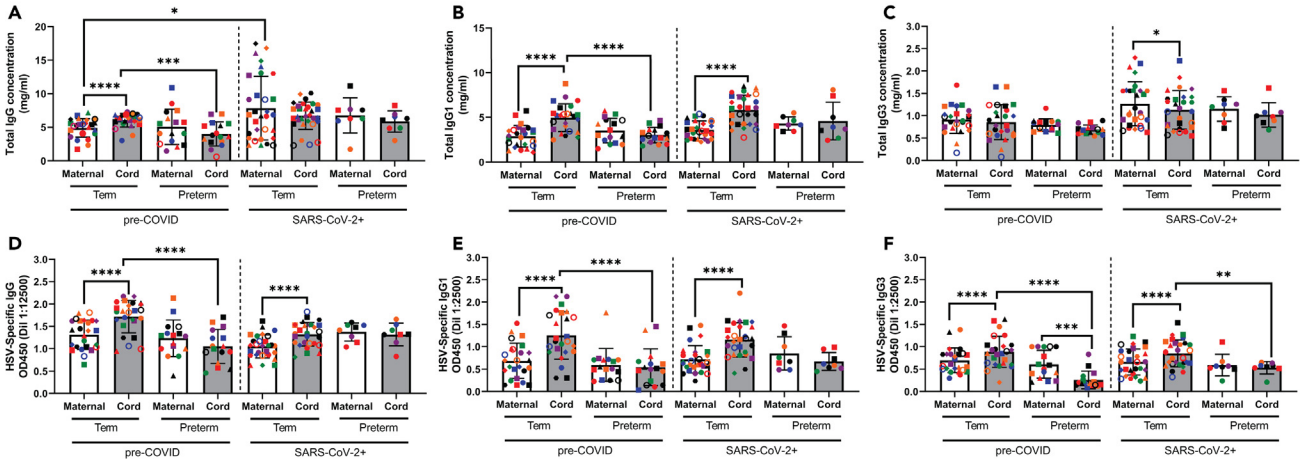

Figure 1. Maternal and cord blood total and HSV-specific IgG in pre-COVID and SARS-CoV-2+ dyads

Total IgG (A), IgG1 (B), and IgG3 (C) and HSV-specific IgG (D), IgG1 (E), and IgG3 (F) were measured in maternal and cord blood for term and preterm pre-COVID and SARS-CoV-2+ dyads. For the HSV-specific Abs, the results are shown as optical densitometry units (odu) at 1:12,500 plasma dilution for IgG and at 1:2500 plasma dilution for IgG1 and IgG3. Each sample was tested in duplicate, and each dyad is color-coded; open symbols indicate dyads where the mother was only HSV-2 seropositive. Maternal and cord blood antibody levels were compared using Wilcoxon matched-pairs signed rank test, and term vs. preterm maternal or cord levels were compared using Mann-Whitney U test (*$p < 0.05$, **$p < 0.01$, ***$p < 0.001$, ****$p < 0.0001$). The bar shows mean ± standard deviation for the group.

There was a statistical differences in the distribution of maternal COVID-19 disease severity comparing the term vs. preterm groups: 17 (60.7%) term and 1 (12.5%) preterm) were asymptomatic and were tested as part of infection control policy; 8 (28.6%) term and 3 (37.5%) preterm were classified with mild disease; 3 (10.7%) term and 2 (25%) preterm were classified with moderate disease; and 2 (25%) preterm mothers had severe disease ($p < 0.05$, chi-square). The onset and duration of SARS-CoV-2 infection is unknown, but all participants had detectable plasma SARS-CoV-2 immunoglobulin M (IgM), immunoglobulin A (IgA), and IgG (Figure S1). None of the mothers had received a COVID-19 vaccine, and none of the newborns were diagnosed with SARS-CoV-2 or neonatal herpes. The majority of pregnant participants were HSV-1+ (n = 61) or HSV-1 and HSV-2 dually seropositive (n = 11), and thus assays were conducted using HSV-1-infected cell lysates or recombinant HSV-1 glycoproteins as antigenic targets. However, as HSV-1 and HSV-2 Abs cross-react, HSV-2-seropositive-only participants (n = 9) were included.

Total and HSV-specific antibody response in mother-infant pre-COVID and SARS-CoV-2+ dyads

Because there was a difference in the timing of maternal blood collection relative to delivery in the pre-COVID term compared to preterm and SARS-CoV-2+ cohorts, we first assessed whether timing was associated with maternal total IgG or HSV-specific IgG. There was no association (Figure S2, $p = 0.31$ and 0.34, respectively). However, the transfer of total IgG and IgG1 (but not IgG3) (Figures 1A–1C) and the transfer of HSV-binding IgG, IgG1, and IgG3 (Figures 1D–1F) were significantly impaired in preterm compared to term pre-COVID dyads with transfer ratios (TRs) (ratio of cord to maternal plasma IgG levels) < 1.0 (Table 2; Figure S3A–S3C). This resulted in significantly less total IgG and IgG1 and HSV-specific IgG, IgG1, and IgG3 in the cord blood of preterm vs. term infants ($p < 0.001$ for total IgG and $p < 0.0001$ for others, Mann-Whitney U test). HSV-specific IgG2 and IgG4 were below the limit of detection in maternal and cord blood and thus were not included in the analyses.

Maternal total IgG concentrations were higher in SARS-CoV-2+ term compared to pre-COVID term or preterm pregnancies (Figure 1A, $p < 0.05$, Kruskal-Wallis with Dunn's multiple comparison test). This was associated with TRs of total IgG <1.0 in both the term and preterm SARS-CoV-2+ cohorts (Table 2). However, similar to the pre-COVID cohort, the TRs of HSV-specific IgG, IgG1, and IgG3 were all significantly lower in preterm versus term SARS-CoV-2+ dyads ($p < 0.001$ for HSV-specific IgG and IgG1, $p < 0.01$ for HSV-specific IgG3, Mann-Whitney U test, Table 2). Inclusion of the few HSV-2 seropositive only, denoted by open symbols (Figure 1), did not impact the results.

Differences in transfer of neutralizing, C1q binding, and FcγRIIIa-activating IgG in term versus preterm pre-COVID and SARS-CoV-2+ dyads

To explore whether there were differences in the function of placentally transferred HSV-specific IgG, we compared the neutralizing titer by plaque reduction assay (Figure 2A), C1q binding activity by ELISA (Figure 2B), and fold activation of human FcγRIIIa (ADCC) (Figure 2C) in paired maternal and cord blood samples using HSV-infected cell lysate as the antigenic target. Activation of FcγRI- and FcγRIIa-activating HSV IgG was also measured, but no increase relative to background was observed.

There were no statistically significant differences in levels of functional Abs comparing mothers who delivered at term vs. preterm. However, the transfer efficiency differed. Neutralizing antibodies (nAbs) were efficiently transported (defined as TR > 1.0) only in term but not preterm dyads (TR 2.44 [1.5–3.3] vs. 0.84 [0.6–1.0], $p < 0.0001$, Mann-Whitney U test, Table 2), which resulted in significantly lower nAb titers in preterm compared to term cord blood (96.57 [45.2–103.7] vs.140.40 [110.5–272.5], $p < 0.01$, Mann-Whitney U test) (Figures 2A and S3D).

Table 2. Transfer ratios of total and HSV-specific IgG (median [IQR])

	pre-COVID			SARS-CoV-2+		
	Term	Preterm	p value	Term	Preterm	p value
IgG[a]	1.17 [1.1–1.4]	0.89 [0.5–1.2]	<0.01	0.96 [0.7–1.2]	087 [0.8–1.1]	NS
IgG1[a]	1.86 [1.3–2.4]	0.92 [0.7–1.1]	<0.0001	1.63 [1.2–2.0]	0.96 [0.7–1.4]	<0.01
IgG3[a]	0.89 [0.6–1.2]	0.99 [0.7–1.1]	NS	0.87 [0.8–1.0]	0.86 [0.6–1.2]	NS
HSV IgG[b]	1.32 [1.2–1.5]	0.85 [0.6–1.2]	<0.0001	1.25 [1.1–1.4]	0.91 [0.8–1.1]	<0.001
HSV IgG1[c]	1.76 [1.5–2.4]	0.90 [0.6–1.1]	<0.0001	1.76 [1.4–2.1]	0.72 [0.6–1.2]	<0.001
HSV IgG3[c]	1.25 [1.1–1.5]	0.42 [0.2–0.8]	<0.0001	1.27 [1.1–1.5]	0.72 [0.6–1.2]	<0.01
Neutralization[d]	2.44 [1.5–3.3]	0.84 [0.6–1.0]	<0.0001	1.44 [1.1–2.2]	0.98 [0.6–1.5]	NS
HSV C1q[e]	1.33 [1.0–2.1]	1.2 [1.0–1.4]	NS	1.06 [1.0–1.5]	1.13 [1.0–1.3]	NS
FcγRIIIa activation[f]	0.72 [0.6–0.8]	0.50 [0.4–0.6]	<0.01	1.20 [1.0–1.4]	0.69 [0.4–1.0]	<0.01
Anti-gD IgG[b]	1.35 [1.2–1.7]			1.40 [1.1–2.4]		NS
Anti-gD IgG1[c]	2.20 [1.6–2.7]			2.10 [1.1–3.1]		NS
Anti-gB IgG[b]	1.45 [1.3–2.3]			2.22 [1.6–3.8]		<0.05
Anti-gB IgG1[c]	2.06 [1.7–2.6]			2.55 [1.9–3.6]		NS
Anti-gB IgG3[c]	1.32 [1.1–1.6]			1.47 [1.3–1.7]		NS

[a]mg/ml.
[b]OD450 at 1:12500 plasma dilution.
[c]OD450 at 1:2500 plasma dilution.
[d]dilution that yielded 50% reduction in viral plaques.
[e]OD450 at 1:20 plasma dilution.
[f]NS = not significant (p > 0.05).

C1q-binding Abs transferred with similar efficiency in term and preterm infants (TR 1.33 [1.0–2.1] and 1.2 [1.0–1.4], respectively; Figure 2B and Table 2). In contrast, FcγRIIIa-activating Abs were inefficiently transferred in both term and preterm dyads, which resulted in significantly lower levels of this functionality in cord compared to maternal plasma ($p < 0.0001$, Figure 2C). The TR was <1.0 in both term and preterm dyads and was significantly lower in the preterm dyads (0.72 [0.6–0.8] vs. 0.50 [0.4–0.6], $p < 0.01$, Mann-Whitney U test, Table 2).

The results for the SARS-CoV-2 maternally coinfected dyads differed from those for the pre-COVID dyads (Figure 2; Table 2). The transfer of nAbs was again greater in term compared to preterm dyads (TR 1.44 [1.1–2.2] vs. 0.98 [0.6–1.5]), but the differences in the TRs were no longer statistically significant. Second and more strikingly, the transfer of FcγRIIIa-activating Abs was significantly greater in term (but not preterm) SARS-CoV-2 dyads compared to pre-COVID dyads (TR 1.20 [1.0–1.4] vs. 0.72 [0.6–0.8], $p < 0.0001$, Kruskal-Wallis with Dunn's multiple comparison test).

Transfer of anti-glycoprotein D (gD)- and anti-glycoprotein B (gB)-specific Abs

The difference in the TR of functionally distinct Abs could reflect their antigenic targets, IgG subclasses, glycans, and/or FcRn affinity. To explore these possibilities, we first compared the transfer of anti-gD and anti-gB Abs using recombinant proteins and plasma from the pre-COVID (Figures 3A and 3C, respectively) and SARS-CoV-2+ (Figures 3B and 3D, respectively) term dyads. These two envelope glycoproteins were selected because both are major targets of nAbs and gB has recently been identified as a target of ADCC responses.[23,33] Both anti-gD and anti-gB IgG were efficiently transported (TR > 1.0, Table 2), but the anti-gD Abs were almost exclusively IgG1 (Figures 3A and 3B) whereas the anti-gB Abs comprised both IgG1 and IgG3 subclasses (Figures 3C and 3D). There were no differences in TR of anti-gD IgG or IgG1 comparing pre-COVID and SARS-CoV-2+ dyads, but the TR of anti-gB IgG was significantly greater in the SARS-CoV-2+ compared to pre-COVID dyads ($p < 0.05$, Mann-Whitney U test) and trended to be higher comparing anti-gB IgG1 and IgG3 subclasses ($p = 0.06$ and $p = 0.09$, Mann-Whitney U test, respectively) (Table 2). These differences are consistent with the higher TR of ADCC-mediating IgG in the SARS-CoV-2+ compared to pre-COVID cohort.

Functionality of antigen- and subclass-enriched Abs in pre-COVID dyads

To further dissect the differences in function of gD- and gB-specific IgG1 and IgG3, we enriched plasma from maternal (n = 4) and cord (n = 3) term pre-COVID samples for anti-glycoprotein-specific IgG using Protein L columns followed by gD and gB lectin columns. The anti-gD-enriched fraction recognized gD (but not gB) on western blots with recombinant proteins or HSV-infected cell lysate as antigens whereas the anti-gB-enriched fraction recognized gB but not gD (Figure S4A). The final flow-through, which was depleted of both anti-gD and anti-gB IgG (gD^-gB^-), recognized several other bands within the HSV-infected lysate but did not recognize recombinant gD or gB protein. The anti-gD IgG had significantly more neutralizing activity compared to either the anti-gB or the gD^-gB^- fraction ($p < 0.001$ and $p < 0.0001$, respectively,

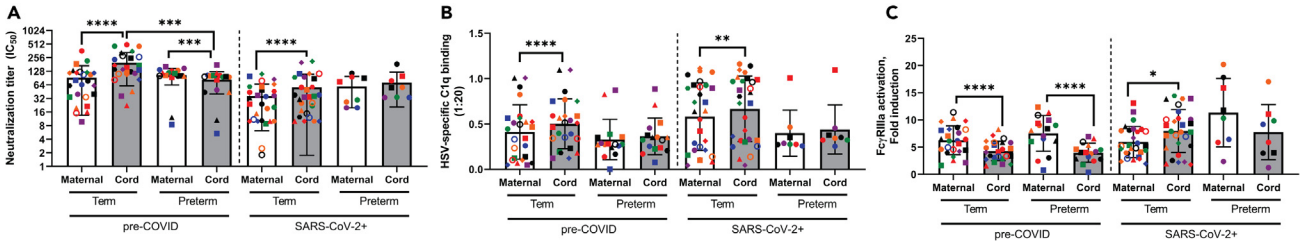

Figure 2. Differences in transfer of neutralizing, C1q-binding, and FcγRIIIa-activating IgG in term versus preterm pre-COVID versus SARS-CoV-2+ dyads

(A) HSV-specific neutralization titers were determined by plaque reduction assay for term and preterm pre-COVID and SARS-CoV-2+ dyads, and results are presented as the plasma dilution that inhibited 50% of viral infection relative to cells infected in the absence of plasma.

(B) HSV-specific C1q-binding Abs were measured by ELISA using HSV-1-infected and uninfected cellular lysate. Results are presented as optical densitometry units (odu) at 1:20 plasma dilution after subtracting the odu response to uninfected cellular lysate.

(C) FcγRIIIa activation was measured using the human FcγRIIIa ADCC Reporter Bioassay with HSV-1-infected cells and 1:5 plasma dilution. Results are presented as fold induction relative to no plasma control. Each sample was tested in duplicate, and each dyad is color-coded; open symbols indicate dyads where the mother was only HSV-2 seropositive. Maternal and cord blood antibody levels were compared using Wilcoxon matched-pairs signed rank test, and term vs. preterm maternal or cord levels were compared using Mann-Whitney U test (*$p < 0.05$, ***$p < 0.001$, ****$p < 0.0001$). The bar shows mean ± standard deviation for the group.

ANOVA with Tukey's multiple comparison) but had little or no FcγRIIIa-activating activity (Figures 4A and 4B). In contrast, the anti-gB and $gD^{-}gB^{-}$ fractions exhibited both functions and had significantly more ADCC-mediating activity compared to the anti-gD-enriched fraction ($p < 0.05$. ANOVA with Tukey's multiple comparisons test). Detection of FcγRIIIa-activating Abs in the $gD^{-}gB^{-}$ fraction is consistent with studies showing that gB is only one of several targets of ADCC-mediating IgG although the other antigenic targets have not been identified.[33]

Given that IgG1 crosses the placenta more efficiently than IgG3 and nAbs cross more efficiently than FcγRIIIa-activating Abs, we hypothesized that the nAbs would be primarily IgG1 whereas the FcγRIIIa-activating Abs might be predominantly IgG3. To test this, we enriched for IgG1 by passing the Protein L column eluent over a Protein A column, which binds IgG1 (as well as IgG2 and IgG4) more efficiently than IgG3;[34] the enrichment was assessed by ELISA with anti-IgG as the capture antigen and subclass-specific secondary Abs (Figure S4B). Refuting our hypothesis, both the neutralizing and the FcγRIII-activating Abs were primarily IgG1 and not IgG3 (Figures 4C and 4D). To confirm this, the anti-gB-enriched IgG (n = 3 pools each comprised plasma from 2 participants) was applied to a Protein A column; the FcγRIIIa activity mapped to the IgG1-enriched fraction (Protein A eluent) (Figure 4E).

The finding that both neutralizing and FcγRIIIa-inducing activity were contained within the IgG1 fractions suggested that the differences in TR might reflect differences in FcRn affinity, which in turn, may be associated with differences in IgG glycan modifications. To assess this, we quantified the apparent affinity for the FcRn. The IgG1 fraction had significantly greater apparent affinity ($1/K_D$) compared to IgG3 ($p < 0.01$, Mann-Whitney U test), and the anti-gD had significantly greater apparent affinity than anti-gB-enriched fractions for the FcRn ($p < 0.0001$, Mann-Whitney U test) (Figure 4F).

Differential expression of glycans in anti-gD- and anti-gB-enriched maternal IgG

MALDI-TOF mass spectrometry analysis of IgG isolated from anti-gD- and anti-gB-enriched fractions (term pre-COVID maternal plasma, n = 5 each) showed increased abundance of terminal sialylated glycans in anti-gD- compared to anti-gB-enriched fractions ($p < 0.01$, paired t test); a modification, when expressed on the Fc region, is associated with FcRn affinity.[7,13,15,35,36] Conversely, the anti-gB-enriched IgG displayed an increased abundance of fucosylated, galactosylated, N-acetylglucosamine (GlcNAc) and bisecting GlcNAc compared to anti-gD (all $p < 0.01$, paired t test, Figure 5A and Table S1). These modifications, when expressed on the Fc, are associated with FcγRIIIa affinity.[7,13,15,36–38] Additional glycan analyses were performed with anti-gD- and anti-gB-enriched IgG from the SARS-CoV-2+ cohort (n = 5 maternal term samples each). Although the trends were similar, no significant differences in the abundance of different glycans were observed comparing the anti-gD- and anti-gB-enriched samples (Figure 5B and Table S1). Moreover, little or no GlcNAc and bisecting GlcNAc glycans were detected in the SARS-CoV-2+ anti-gD- or anti-gB-enriched samples. These findings suggest that differences in glycans alone do not explain the increased TR of FcγRIIIa-activating IgG in the term SARS-CoV-2+ cohort.

Increased colocalization of FcRn and FcγRIIIa on placentas from SARS-CoV-2-positive mothers compared to SARS-CoV-2-negative mothers

To determine if placental expression of FcRn or FcγRIIIa contributed to increased transfer of ADCC-mediating IgG, placental tissue from SARS-CoV-2+ and contemporaneous SARS-CoV-2 PCR negative (SARS-CoV-2-) deliveries (n = 8 term and n = 5 preterm each) were stained with Abs to placental alkaline phosphatase (PLAP), FcRn, and FcγRIIIa and the expression and colocalization compared (Figure 6). As expected, there was significantly more staining of FcRn in term compared to preterm placental tissue independent of SARS-CoV-2 coinfection ($p < 0.01$ for SARS-CoV-2- and $p < 0.05$ for SARS-CoV-2+, Kruskal-Wallis with Dunn's multiple comparison test, Figure 6B). There was no difference in relative amount of FcγRIIIa staining, but FcRn-FcγRIIIa colocalization was greatest in the term SARS-CoV-2+ placental tissue and

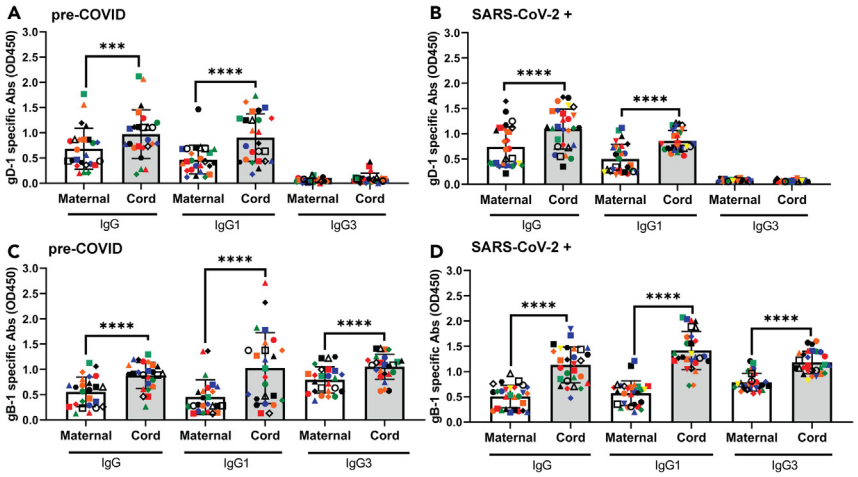

Figure 3. Transfer of anti-glycoprotein D- and anti-glycoprotein B-specific Abs

The relative concentrations of anti-gD- (A and B) and anti-gB (C and D)-specific IgG, IgG1, and IgG3 were quantified in term pre-COVID (A and C) and SARS-CoV-2+ (B and D) dyads by ELISA with recombinant proteins as antigens in paired samples from term dyads. Results are presented as odu at 1:12500 plasma dilution for IgG and at 1:2500 plasma dilution for IgG1 and IgG3. Each symbol is the mean of duplicates, and each dyad is color-coded; open symbols indicate dyads from HSV-2 seropositive only mothers (Wilcoxon matched-pairs signed rank test, ***$p < 0.001$, ****$p < 0.0001$). The bar shows mean ± standard deviation for the group.

was significantly greater than that in term and preterm SARS-CoV-2- tissue ($p < 0.05$ and $p < 0.01$, Kruskal-Wallis with Dunn's multiple comparison test, respectively, Figures 6C and 6D).

Multivariable analyses confirm association of gestational age and SARS-CoV-2 coinfection with transfer of neutralizing and FcγRIIIa-activating IgG, respectively

Multivariable linear regression models were constructed to identify factors associated with transfer of HSV-specific IgG, neutralizing, or FcγRIIIa-activating Abs. Variables included maternal age, neonatal sex, gestational age (dichotomized as term vs. preterm), COVID-19 infection, timing of maternal blood collection, maternal total IgG, and HSV-specific IgG. Gestational age and maternal HSV-specific IgG levels were associated with the transfer of HSV-specific IgG (both $p < 0.0001$). Gestational age was also positively associated with the transfer of nAbs ($p < 0.03$). In contrast, COVID-19 infection and newborn female sex were significantly associated with the transfer of FcγRIIIa-activating Abs. However, the interaction between neonatal sex and COVID-19 was significant ($p < 0.05$), and when this was included in the model, only COVID-19 status retained a significant association ($p < 0.05$, Table 3). Moreover, when only female newborns were included in the model, COVID-19 infection was positively associated with FcγRIIIa-activating Ab transfer ($p < 0.05$), but the association was not significant when only males were included (Table S2). We further assessed the potential association between timing of maternal blood collection and TRs. There was no significant association between maternal blood collection time (relative to delivery) and TR of HSV-specific IgG (rho = 0.15m, $p = 0.18$), nAbs (rho = 0.29, $p = 0.35$), or ADCC-mediating Abs (rho = −0.11, $p = 0.32$) (Figure S5).

DISCUSSION

Results of these studies demonstrate that preterm vs. term gestation, antibody function, IgG glycans, and placental expression and colocalization of FcRn and FcγRIIIa contribute to efficiency of HSV-specific IgG placental transfer. The transfer of nAbs, which are the dominant response to acute HSV infection,[39] is greater than FcγRIIIa-activating and C1q-binding Abs in term pre-COVID dyads as reflected by the differences in TRs. The relative inefficient transfer (TR < 1.0) of FcγRIIIa-activating, ADCC-mediating IgG in both term and preterm neonates (in the absence of SARS-CoV-2 coinfection) may have important clinical implications since, as suggested by a prior clinical study, ADCC likely plays a more important role in controlling viral dissemination.[22] The importance of ADCC in protecting neonates has also been suggested in mouse studies, which demonstrated that immunization of female mice with a vaccine that elicits a predominant ADCC response protected their pups from subsequent viral challenge whereas nAbs elicited by HSV infection or a gD subunit vaccine were less protective.[32,40] Preterm infants may be particularly vulnerable to disease because the transfer of both neutralizing and ADCC-mediating IgG is compromised (TR < 1.0). The importance of gestational age in modifying transfer of neutralizing IgG (but not FcγRIIIa-activating IgG) was confirmed in the multivariable linear regression model where gestational age was the only significantly associated factor. This is likely a consequence of decreased expression of the FcRn in preterm placentas, which we documented by immunohistochemistry, as well as shorter time available for Abs to cross.

Differences in IgG subclass do not explain the differential placental transfer of neutralizing compared to FcγRIIIa-activating Abs as both were predominantly IgG1; the anti-gD IgG were restricted to the IgG1 subclass, and while anti-gB included both IgG1 and IgG3, all the

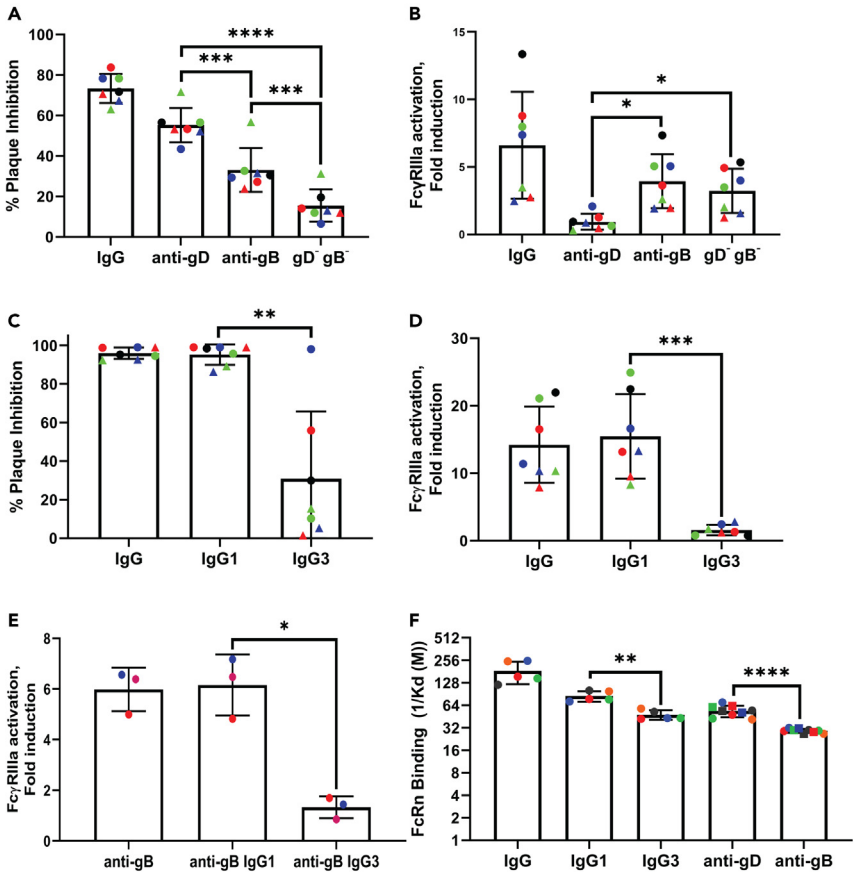

Figure 4. Functionality of antigen- and subclass-enriched Abs in pre-COVID dyads

Maternal (n = 4, circles) and cord (n = 3, triangles) term pre-COVID plasma was enriched for anti-gD and anti-gB or IgG1 and IgG3 subclasses and then assayed for neutralization activity (A and C) or FcγRIIIa activation (B and D) using 0.5 mg/mL of each enriched sample. Each sample was tested in duplicate. Neutralization is presented as the percent reduction in viral plaque formation relative to control wells.

(E) Additional pooled samples (n = 3 pools from 2 participants each) were sequentially passaged over the gB lectin followed by Protein A columns and assayed using the ADCC reporter assay at 0.5 mg/mL.

(F) The relative FcRn-binding affinity of enriched samples was measured using Lumit FcRn binding assay, and results are shown as relative apparent affinity ($1/K_D$ [M]). The bars indicate mean ± standard deviation. Differences between anti-gD, anti-gB, and gD^-gB^- neutralization and FcγRIIIa activation were compared using ANOVA with Tukey's multiple comparison (A and B), and differences between IgG1 and IgG3 or anti-gD and anti-gB in C–F were compared by Mann-Whitney U test (*p < 0.05, **p < 0.01, ***p < 0.001, ****p < 0.0001).

ADCC-mediating activity mapped to IgG1. However, the antigenic targets and glycans differed, and we speculate that this may have contributed to the variance in transfer efficiency. The anti-gD Abs had essentially only neutralizing activity, had greater apparent affinity ($1/K_D$) for FcRn, and expressed glycans that, when expressed on the Fc region, are associated with increased FcRn affinity. In contrast, the anti-gB IgG exhibited both neutralizing and FcγRIIIa-activating functions and expressed relatively more glycans, which when expressed on the Fc region, are associated with greater FcγRIIIa affinity. Although we separated the anti-gB IgG1 from IgG3 to confirm that the FcγRIIIa-activating function mapped to IgG1, we were unable to separate the neutralizing from FcγRIIIa-activating anti-gB IgG1 for glycan studies. Moreover, we conducted the glycan studies with total IgG and thus could not distinguish Fc from Fab glycans. While most studies that associated N-linked glycans with FcR affinity focus only on Fc glycans, Fab domain glycans can also modulate placental transfer efficiency. Based on our findings, we speculate that the anti-gB with neutralizing activity would express relatively more terminal Fc sialylated glycans and the ADCC-mediating anti-gB more fucosylated, bisecting GlcNAs and digalactosylated glycans reflecting different relative affinities for FcRn and FcγRIIIa, respectively.[7,13,15,35–37,41–44]

SARS-CoV-2 coinfection was associated with a significant increase in the transfer of FcγRIIIa-activating Abs and a concomitant small decrease in the transfer of nAbs. This increase was significant comparing the term SARS-CoV-2+ dyads to all the other groups. This finding was unanticipated as infections including SARS-CoV-2, HIV, and malaria, for example, are more often associated with decreased IgG transport.[13,25,27] The proposed mechanisms for impaired transport in the setting of maternal coinfections include hypergammaglobulinemia (IgG >15 g/L) with associated saturation of placental FcRn, alterations in glycans, and inflammatory changes in the placenta.[13,25] While we did observe a modest increase in total IgG in the SARS-CoV-2+ mothers, this increase was not sufficient to saturate receptors or decrease the

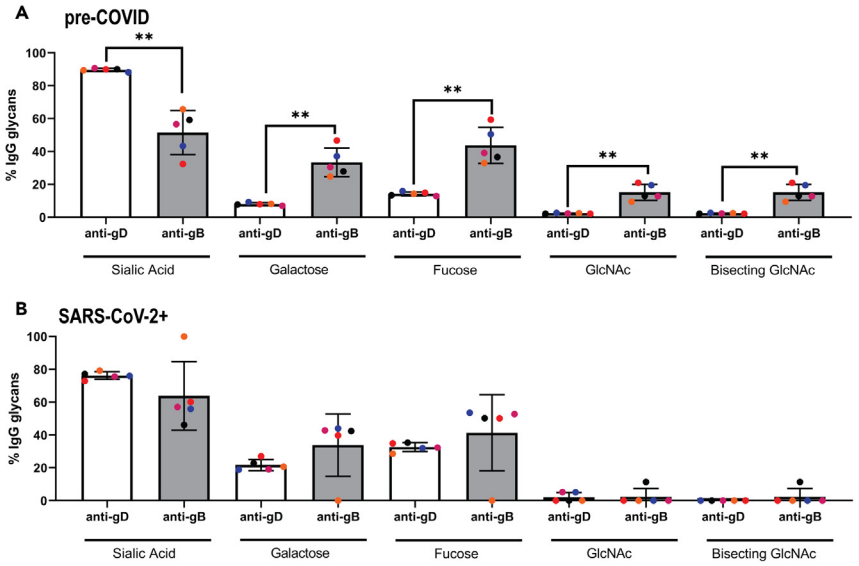

Figure 5. Differential expression of glycans in anti-glycoprotein D- and anti-glycoprotein B-enriched maternal IgG

The relative glycan composition of anti-glycoprotein D- and anti-glycoprotein B-enriched plasma were quantified by mass spectrometry in samples from pre-COVID (A) and SARS-CoV-2+ (B) mothers who delivered at term (n = 5 each). The relative abundance of glycans expressing sialic acid, galactose, fucose, GlcNAc, and bisecting GlcNAc was calculated. Each symbol is the mean of duplicates, and each sample is color-coded. The bars indicate mean ± standard deviation for the group, and the abundance of glycans in the anti-gD- versus anti-gB-enriched samples is compared by paired t test (**p < 0.01).

TR of HSV-specific IgG. There were also differences in glycans with a decrease in GlcNAc and bisecting GlcNAc glycans in the anti-gB-enriched SARS-CoV-2 compared to pre-COVID dyads. However, this difference is unlikely to contribute to the observed increase in transfer of ADCC-mediating IgG. Rather, we speculate that the increased colocalization of FcRn and FcγRIIIa observed in the immunohistochemistry studies of placental tissue obtained from SARS-CoV-2+ compared to SARS-CoV-2- term deliveries facilitated the transfer of ADCC-mediating IgG. This finding is consistent with another recent study that also documented increased FcRn/FcγRIIIa colocalization, which could favor the transfer of IgG with increased affinity for the FcγRIIIa.[25] How SARS-CoV-2 infection modifies placental architecture and whether similar changes occur in response to other active infections require future study.

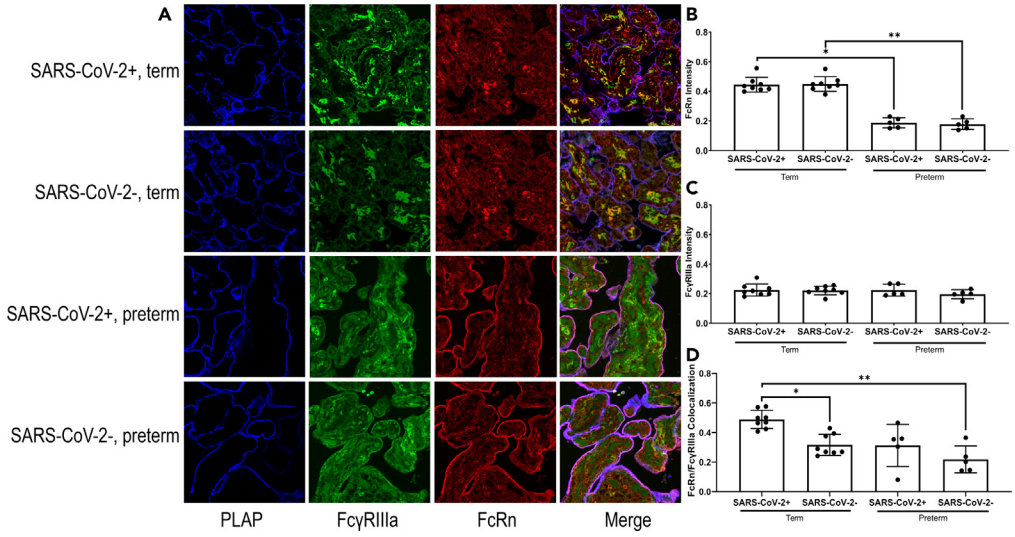

Figure 6. Increased colocalization of FcRn and FcγRIIIa on placentas from SARS-CoV-2-positive mothers compared to SARS-CoV-2-negative mothers

Immunohistochemistry was performed on placental tissues obtained from SARS-CoV-2-positive and negative mothers (n = 8 each for Term and n = 5 for preterm) and stained for placental alkaline phosphatase (PLAP), FcRn and FcγRIIIa. (A) Representative slides from one term and preterm SARS-CoV-2-positive and negative placenta each are shown. Intensity of FcRn (B), FcγRIIIa (C), and colocalization of these (D) were quantified using ImageJ (FcRn intensities were compared using Kruskal-Wallis with Dunn's multiple comparison, *p < 0.05, **p < 0.01).

Table 3. Variables associated with transfer ratios of HSV-specific IgG, neutralizing, or FcγRIIIa-activating Abs using linear regression models

Dependent variable	HSV-specific IgG		Neutralization titer		FcγRIIIa activation	
Model R^2 (p value)	0.50 (0.00001)		0.23 (0.03)		0.47 (0.00001)	
	β-coefficient ±SE	p value	β-coefficient ± SE	p value	β-coefficient ± SE	p value
Neonatal Sex	0.10 ± 0.06	0.1	−0.1 ± 0.4	0.7	0.11 ± 0.2	0.2
Gestational age	0.04 ± 0.01	0.0001	0.1 ± 0.1	0.03	0.01 ± 0.3	0.6
COVID Infection	−0.01 ± 0.1	0.9	−0.1 ± 0.6	0.7	0.7 ± 0.3	0.03
Maternal IgG	−0.02 ± 0.01	0.07	−0.13 ± 0.07	0.05	−0.04 ± 0.03	0.2
Maternal HSV IgG	−0.45 ± 0.1	0.0001	−0.9 ± 0.07	0.2	−0.41 ± 0.3	0.14
Maternal age	0.01 ± 0.001	0.3	0.04 ± 0.04	0.3	0.01 ± 0.01	0.4
Time from sample collection till delivery	0.002 ± 0.001	0.3	−0.005 ± 0.01	0.7	0.003 ± 0.005	0.5
Constant	0.28 ± 0.4	0.5	−2.5 ± 2.9	0.4	−0.60 ± 1.2	0.6
Sex: COVID-19[a]					0.41 ± 0.3	0.02

[a]Measure of interaction between neonatal sex and COVID status.

Notably, there was a significant interaction between female neonatal sex and COVID-19 infection, resulting in increased transfer of FcγRIIIa-activating IgG in female SARS-CoV-2+ dyads. Relatively greater placental transfer of maternal IgG in female versus male newborns was previously reported in a SARS-CoV-2+ cohort and was linked in part to reduced maternal IgG levels.[45] However, we did not observe differences in maternal HSV-specific IgG when comparing male versus female pregnancies and there were no sex-based differences in placental FcRn/FcγRIIIa expression although the sample size is small. Thus, the underlying mechanisms for this association require future investigation.

The observation that HSV-specific FcγRIIIa-activating Abs (in the absence of SARS-CoV-2 coinfection) are transmitted inefficiently (TR < 1.0) contrasts with findings showing selective transfer of FcγRIIIa-activating Abs targeting pertussis, influenza, and respiratory syncytial virus (RSV) antigens (TR > 1.0).[15] The differences may be linked to differential glycan expression as the anti-gB IgG expressed significantly less galactosylated glycans whereas the anti-RSV and anti-influenza IgG in the prior study expressed increased levels of galactosylated glycans, which are associated with FcRn and FcγRIIIa binding.[14,15]

In summary, the results of this study on placental transfer of HSV-specific IgG have several potential clinical implications. The relative inefficient transfer of ADCC-mediating Abs (in the absence of SARS-CoV-2 coinfection), combined with the prior observation that only low levels of ADCC-mediating Abs are elicited in response to primary HSV infection,[23] may contribute to the increased risk of neonatal disease associated with primary maternal infection. If ADCC is important for preventing neonatal herpes dissemination,[22] vaccines that elicit high titer ADCC responses and monoclonal Abs with ADCC-mediating activity including those that target gB[33] should be prioritized. The monoclonal Abs should be engineered to express glycans that promote both FcRn binding and FcγRIII activation to optimize placental transfer. Future studies should also focus on understanding the mechanisms that promote FcRn and FcγRIII colocalization as potential strategies to promote antibody transfer.

Limitations of the study

There are several limitations to this study including the absence of any HSV transmission and the recruitment of pre-COVID and SARS-CoV-2+ cohorts during different time periods. However, it would have been difficult to identify SARS-CoV-2-uninfected pregnancies during the first wave of the pandemic. Another limitation is that the time between maternal blood collection and delivery differed for the pre-COVID term and the other groups. Almost all the pregnant women recruited earlier in the third trimester delivered at term. However, the multivariable models as well as lack of any significant association (Spearman correlation) between timing of maternal blood collection and maternal antibody titers or TRs strongly suggest that this difference did not impact the results. In addition, we evaluated Abs directed against only two viral antigens, gB and gD. While these accounted for the majority of nAbs, the anti-gD- and anti-gB-depleted fraction retained substantial ADCC-mediating activity. Identification of the targets and placental transfer efficiency of these potentially functionally important Abs requires future study. In addition, the glycan studies were conducted only with maternal samples and not with isolated Fc fragments. Glycans expressed by Fab and Fc may contribute to antibody function, conformation, affinity for the FcRn, and placental transfer. Future more detailed analyses of isolated Fc glycans as well as glycans in the cord blood are needed to establish the link between glycans and placental transfer.

STAR★METHODS

Detailed methods are provided in the online version of this paper and include the following:

- KEY RESOURCES TABLE
- RESOURCE AVAILABILITY
  - Lead contact

SUPPLEMENTAL INFORMATION

Supplemental information can be found online at https://doi.org/10.1016/j.isci.2023.107648.

ACKNOWLEDGMENTS

The authors thank Anayeli Correa for her assistance with ELISA's, Benjamin Galen and the nurses and residents from OB-GYN Montefiore for their assistance with patient recruitment and sample collection, Tao Wang for his assistance with statistics, Scott Garforth and Steve Almo for providing gB and gD proteins, Einstein Pathology for providing placental tissue, and Andrea Briceno from Einstein Analytical Imaging Facility and Danielle Rayee for their assistance with immunohistochemistry and confocal imagining. We also thank the patients for their participation in the study. The authors would also like to acknowledge funding received from multiple sources: National Institutes of Health R01AI134367 (BCH), R21AI147992 (SP and BCH), R01HD098977 (BCH), P30AI124414 (BCH), Price Family Foundation (BCH), CTSA training grant (TL1 TR002557) (AMM), NIH Office of the Director (1-S10-OD030286-01) (SS), Einstein Cancer Center (P30-CA013330) (SS), and Shared Instrumentation Grant (SIG) # 1S10OD023591-01 (Analytic Imaging Facility).

AUTHOR CONTRIBUTIONS

AMM, FET, and BCH designed the study; AMM and FET recruited patients and collected samples; AMM, JTA, and SS performed experiments and performed data analysis; AMM, SRP, and BCH wrote the manuscript, and all authors edited the manuscript.

DECLARATION OF INTERESTS

Dr. Herold receives support and serves on the Scientific Advisory Board of X-Vax, Technologies. Dr. Herold is also an inventor on patents for the development of ΔgD-2 vaccine and a pending application for HSV-specific monoclonal Abs for prevention and treatment of herpes simplex virus infections.

Received: March 20, 2023
Revised: May 30, 2023
Accepted: August 11, 2023
Published: August 15, 2023

REFERENCES

1. Marshall, H., McMillan, M., Andrews, R.M., Macartney, K., and Edwards, K. (2016). Vaccines in pregnancy: The dual benefit for pregnant women and infants. Hum. Vaccin. Immunother. *12*, 848–856. https://doi.org/10.1080/21645515.2015.1127485.
2. Lindsey, B., Kampmann, B., and Jones, C. (2013). Maternal immunization as a strategy to decrease susceptibility to infection in newborn infants. Curr. Opin. Infect. Dis. *26*, 248–253. https://doi.org/10.1097/QCO.0b013e3283607a58.
3. Halasa, N.B., Olson, S.M., Staat, M.A., Newhams, M.M., Price, A.M., Pannaraj, P.S., Boom, J.A., Sahni, L.C., Chiotos, K., Cameron, M.A., et al. (2022). Maternal Vaccination and Risk of Hospitalization for Covid-19 among Infants. N. Engl. J. Med. *387*, 109–119. https://doi.org/10.1056/NEJMoa2204399.
4. Sakala, I.G., Honda-Okubo, Y., Fung, J., and Petrovsky, N. (2016). Influenza immunization during pregnancy: Benefits for mother and infant. Hum. Vaccin. Immunother. *12*, 3065–3071. https://doi.org/10.1080/21645515.2016.1215392.
5. Perrett, K.P., Halperin, S.A., Nolan, T., Carmona Martínez, A., Martinón-Torres, F., García-Sicilia, J., Virta, M., Vanderkooi, O.G., Zuccotti, G.V., Manzoni, P., et al. (2020). Impact of tetanus-diphtheria-acellular pertussis immunization during pregnancy on subsequent infant immunization seroresponses: follow-up from a large randomized placebo-controlled trial. Vaccine *38*, 2105–2114. https://doi.org/10.1016/j.vaccine.2019.10.104.
6. Halasa, N.B., Olson, S.M., Staat, M.A., Newhams, M.M., Price, A.M., Boom, J.A., Sahni, L.C., Cameron, M.A., Pannaraj, P.S., Bline, K.E., et al. (2022). Effectiveness of Maternal Vaccination with mRNA COVID-19 Vaccine During Pregnancy Against COVID-19-Associated Hospitalization in Infants Aged <6 Months - 17 States, July 2021-January 2022. MMWR Morb. Mortal. Wkly. Rep. *71*, 264–270. https://doi.org/10.15585/mmwr.mm7107e3.
7. Palmeira, P., Quinello, C., Silveira-Lessa, A.L., Zago, C.A., and Carneiro-Sampaio, M. (2012). IgG placental transfer in healthy and pathological pregnancies. Clin. Dev. Immunol. *2012*, 985646. https://doi.org/10.1155/2012/985646.
8. Dolatshahi, S., Butler, A.L., Pou, C., Henckel, E., Bernhardsson, A.K., Gustafsson, A., Bohlin, K., Shin, S.A., Lauffenburger, D.A., Brodin, P., and Alter, G. (2022). Selective transfer of maternal antibodies in preterm

and fullterm children. Sci. Rep. *12*, 14937. https://doi.org/10.1038/s41598-022-18973-4.
9. Neuber, T., Frese, K., Jaehrling, J., Jäger, S., Daubert, D., Felderer, K., Linnemann, M., Höhne, A., Kaden, S., Kölln, J., et al. (2014). Characterization and screening of IgG binding to the neonatal Fc receptor. mAbs *6*, 928–942. https://doi.org/10.4161/mabs.28744.
10. Wilcox, C.R., Holder, B., and Jones, C.E. (2017). Factors Affecting the FcRn-Mediated Transplacental Transfer of Antibodies and Implications for Vaccination in Pregnancy. Front. Immunol. *8*, 1294. https://doi.org/10.3389/fimmu.2017.01294.
11. Dashivets, T., Thomann, M., Rueger, P., Knaupp, A., Buchner, J., and Schlothauer, T. (2015). Multi-Angle Effector Function Analysis of Human Monoclonal IgG Glycovariants. PLoS One *10*, e0143520. https://doi.org/10.1371/journal.pone.0143520.
12. Bas, M., Terrier, A., Jacque, E., Dehenne, A., Pochet-Béghin, V., Beghin, C., Dezetter, A.S., Dupont, G., Engrand, A., Beaufils, B., et al. (2019). Fc Sialylation Prolongs Serum Half-Life of Therapeutic Antibodies. J. Immunol. *202*, 1582–1594. https://doi.org/10.4049/jimmunol.1800896.
13. Martinez, D.R., Fong, Y., Li, S.H., Yang, F., Jennewein, M.F., Weiner, J.A., Harrell, E.A., Mangold, J.F., Goswami, R., Seage, G.R., 3rd, et al. (2019). Fc Characteristics Mediate Selective Placental Transfer of IgG in HIV-Infected Women. Cell *178*, 190–201.e11. https://doi.org/10.1016/j.cell.2019.05.046.
14. Vidarsson, G., Dekkers, G., and Rispens, T. (2014). IgG subclasses and allotypes: from structure to effector functions. Front. Immunol. *5*, 520. https://doi.org/10.3389/fimmu.2014.00520.
15. Jennewein, M.F., Goldfarb, I., Dolatshahi, S., Cosgrove, C., Noelette, F.J., Krykbaeva, M., Das, J., Sarkar, A., Gorman, M.J., Fischinger, S., et al. (2019). Fc Glycan-Mediated Regulation of Placental Antibody Transfer. Cell *178*, 202–215.e14. https://doi.org/10.1016/j.cell.2019.05.044.
16. James, S.H., and Kimberlin, D.W. (2015). Neonatal herpes simplex virus infection: epidemiology and treatment. Clin. Perinatol. *42*, 47–59. viii. https://doi.org/10.1016/j.clp.2014.10.005.
17. Pinninti, S.G., and Kimberlin, D.W. (2018). Neonatal herpes simplex virus infections. Semin. Perinatol. *42*, 168–175. https://doi.org/10.1053/j.semperi.2018.02.004.
18. Brown, Z.A., Wald, A., Morrow, R.A., Selke, S., Zeh, J., and Corey, L. (2003). Effect of serologic status and cesarean delivery on transmission rates of herpes simplex virus from mother to infant. JAMA *289*, 203–209. https://doi.org/10.1001/jama.289.2.203.
19. Looker, K.J., Magaret, A.S., May, M.T., Turner, K.M.E., Vickerman, P., Newman, L.M., and Gottlieb, S.L. (2017). First estimates of the global and regional incidence of neonatal herpes infection. Lancet Global Health *5*, e300–e309. https://doi.org/10.1016/S2214-109X(16)30362-X.
20. Corey, L., and Wald, A. (2009). Maternal and neonatal herpes simplex virus infections. N. Engl. J. Med. *361*, 1376–1385. https://doi.org/10.1056/NEJMra0807633.
21. Estrada, F., Mahant, A.M., Guerguis, S., Sy, S., Lu, C., Reznik, S.E., and Herold, B.C. (2023). Prolonged Preterm Rupture of Membranes Associated with Neonatal Disseminated Herpes Simplex Virus Type 1 at Birth: Is There a Role for Preemptive Test and Treat Strategies in High-Risk Populations? J. Pediatric Infect. Dis. Soc. *12*, 246–247. https://doi.org/10.1093/jpids/piac131.
22. Kohl, S., West, M.S., Prober, C.G., Sullender, W.M., Loo, L.S., and Arvin, A.M. (1989). Neonatal antibody-dependent cellular cytotoxic antibody levels are associated with the clinical presentation of neonatal herpes simplex virus infection. J. Infect. Dis. *160*, 770–776. https://doi.org/10.1093/infdis/160.5.770.
23. Mahant, A.M., Guerguis, S., Blevins, T.P., Cheshenko, N., Gao, W., Anastos, K., Belshe, R.B., and Herold, B.C. (2022). Failure of Herpes Simplex Virus Glycoprotein D Antibodies to Elicit Antibody-Dependent Cell-Mediated Cytotoxicity: Implications for Future Vaccines. J. Infect. Dis. *226*, 1489–1498. https://doi.org/10.1093/infdis/jiac284.
24. Englund, J.A. (2007). The influence of maternal immunization on infant immune responses. J. Comp. Pathol. *137* (*Suppl 1*), S16–S19. https://doi.org/10.1016/j.jcpa.2007.04.006.
25. Atyeo, C., Pullen, K.M., Bordt, E.A., Fischinger, S., Burke, J., Michell, A., Slein, M.D., Loos, C., Shook, L.L., Boatin, A.A., et al. (2021). Compromised SARS-CoV-2-specific placental antibody transfer. Cell *184*, 628–642.e10. https://doi.org/10.1016/j.cell.2020.12.027.
26. Farquhar, C., Nduati, R., Haigwood, N., Sutton, W., Mbori-Ngacha, D., Richardson, B., and John-Stewart, G. (2005). High maternal HIV-1 viral load during pregnancy is associated with reduced placental transfer of measles IgG antibody. J. Acquir. Immune Defic. Syndr. *40*, 494–497. https://doi.org/10.1097/01.qai.0000168179.68781.95.
27. Okoko, B.J., Wesuperuma, L.H., Ota, M.O., Banya, W.A., Pinder, M., Gomez, F.S., Osinusi, K., and Hart, A.C. (2001). Influence of placental malaria infection and maternal hypergammaglobulinaemia on materno-foetal transfer of measles and tetanus antibodies in a rural west African population. J. Health Popul. Nutr. *19*, 59–65.
28. Burn Aschner, C., Knipe, D.M., and Herold, B.C. (2020). Model of vaccine efficacy against HSV-2 superinfection of HSV-1 seropositive mice demonstrates protection by antibodies mediating cellular cytotoxicity. NPJ Vaccines *5*, 35. https://doi.org/10.1038/s41541-020-0184-7.
29. Burn Aschner, C., Loh, L.N., Galen, B., Delwel, I., Jangra, R.K., Garforth, S.J., Chandran, K., Almo, S., Jacobs, W.R., Jr., Ware, C.F., and Herold, B.C. (2020). HVEM signaling promotes protective antibody-dependent cellular cytotoxicity (ADCC) vaccine responses to herpes simplex viruses. Sci. Immunol. *5*, eaax2454. https://doi.org/10.1126/sciimmunol.aax2454.
30. Burn Aschner, C., Pierce, C., Knipe, D.M., and Herold, B.C. (2020). Vaccination Route as a Determinant of Protective Antibody Responses against Herpes Simplex Virus. Vaccines (Basel) *8*, 277. https://doi.org/10.3390/vaccines8020277.
31. Burn, C., Ramsey, N., Garforth, S.J., Almo, S., Jacobs, W.R., Jr., and Herold, B.C. (2018). A Herpes Simplex Virus (HSV)-2 Single-Cycle Candidate Vaccine Deleted in Glycoprotein D Protects Male Mice From Lethal Skin Challenge With Clinical Isolates of HSV-1 and HSV-2. J. Infect. Dis. *217*, 754–758. https://doi.org/10.1093/infdis/jix628.
32. Kao, C.M., Goymer, J., Loh, L.N., Mahant, A., Burn Aschner, C., and Herold, B.C. (2020). Murine Model of Maternal Immunization Demonstrates Protective Role for Antibodies That Mediate Antibody-Dependent Cellular Cytotoxicity in Protecting Neonates From Herpes Simplex Virus Type 1 and Type 2. J. Infect. Dis. *221*, 729–738. https://doi.org/10.1093/infdis/jiz521.
33. Kuraoka, M., Aschner, C.B., Windsor, I.W., Mahant, A.M., Garforth, S.J., Kong, S.L., Achkar, J.M., Almo, S.C., Kelsoe, G., and Herold, B.C. (2023). A non-neutralizing glycoprotein B monoclonal antibody protects against herpes simplex virus disease in mice. J. Clin. Invest. *133*, e161968. https://doi.org/10.1172/JCI161968.
34. Kronvall, G., and Williams, R.C., Jr. (1969). Differences in anti-protein A activity among IgG subgroups. J. Immunol. *103*, 828–833.
35. Jennewein, M.F., and Alter, G. (2017). The Immunoregulatory Roles of Antibody Glycosylation. Trends Immunol. *38*, 358–372. https://doi.org/10.1016/j.it.2017.02.004.
36. Einarsdottir, H.K., Selman, M.H.J., Kapur, R., Scherjon, S., Koeleman, C.A.M., Deelder, A.M., van der Schoot, C.E., Vidarsson, G., and Wuhrer, M. (2013). Comparison of the Fc glycosylation of fetal and maternal immunoglobulin G. Glycoconj. J. *30*, 147–157. https://doi.org/10.1007/s10719-012-9381-6.
37. Jansen, B.C., Bondt, A., Reiding, K.R., Lonardi, E., de Jong, C.J., Falck, D., Kammeijer, G.S.M., Dolhain, R.J.E.M., Rombouts, Y., and Wuhrer, M. (2016). Pregnancy-associated serum N-glycome changes studied by high-throughput MALDI-TOF-MS. Sci. Rep. *6*, 23296. https://doi.org/10.1038/srep23296.
38. Pucic, M., Knezevic, A., Vidic, J., Adamczyk, B., Novokmet, M., Polasek, O., Gornik, O., Supraha-Goreta, S., Wormald, M.R., Redzic, I., et al. (2011). High throughput isolation and glycosylation analysis of IgG-variability and heritability of the IgG glycome in three isolated human populations. Mol. Cell. Proteomics *10*. M111.010090. https://doi.org/10.1074/mcp.M111.010090.
39. Mahant, A.M., Guerguis, S., Blevins, T.P., Cheshenko, N., Gao, W., Anastos, K., Belshe, R.B., and Herold, B.C. (2022). Herpes Simplex Virus Glycoprotein D Antibodies Fail to Elicit Antibody-Dependent Cell-Mediated Cytotoxicity: Implications for Future Vaccines. J. Infect. Dis. *226*, 1489–1498. https://doi.org/10.1093/infdis/jiac284.
40. Kohl, S., Strynadka, N.C., Hodges, R.S., and Pereira, L. (1990). Analysis of the role of antibody-dependent cellular cytotoxic antibody activity in murine neonatal herpes simplex virus infection with antibodies to synthetic peptides of glycoprotein D and monoclonal antibodies to glycoprotein B. J. Clin. Invest. *86*, 273–278. https://doi.org/10.1172/JCI114695.
41. Jansen, B.C., Bondt, A., Reiding, K.R., Scherjon, S.A., Vidarsson, G., and Wuhrer, M. (2016). MALDI-TOF-MS reveals differential N-linked plasma- and IgG-glycosylation profiles between mothers and their newborns. Sci. Rep. *6*, 34001. https://doi.org/10.1038/srep34001.
42. Arnold, J.N., Wormald, M.R., Sim, R.B., Rudd, P.M., and Dwek, R.A. (2007). The impact of glycosylation on the biological function and structure of human immunoglobulins. Annu. Rev. Immunol. *25*, 21–50. https://doi.org/10.1146/annurev.immunol.25.022106.141702.

43. Hiatt, A., Bohorova, N., Bohorov, O., Goodman, C., Kim, D., Pauly, M.H., Velasco, J., Whaley, K.J., Piedra, P.A., Gilbert, B.E., and Zeitlin, L. (2014). Glycan variants of a respiratory syncytial virus antibody with enhanced effector function and *in vivo* efficacy. Proc. Natl. Acad. Sci. USA *111*, 5992–5997. https://doi.org/10.1073/pnas.1402458111.

44. Volkov, M., Brinkhaus, M., van Schie, K.A., Bondt, A., Kissel, T., van der Kooi, E.J., Bentlage, A.E.H., Koeleman, C.A.M., de Taeye, S.W., Derksen, N.I., et al. (2023). IgG Fab Glycans Hinder FcRn-Mediated Placental Transport. J. Immunol. *210*, 158–167. https://doi.org/10.4049/jimmunol.2200438.

45. Bordt, E.A., Shook, L.L., Atyeo, C., Pullen, K.M., De Guzman, R.M., Meinsohn, M.C., Chauvin, M., Fischinger, S., Yockey, L.J., James, K., et al. (2021). Maternal SARS-CoV-2 infection elicits sexually dimorphic placental immune responses. Sci. Transl. Med. *13*, eabi7428. https://doi.org/10.1126/scitranslmed.abi7428.

46. World Health Organization (2020). Living Guidance for Clinical Management of COVID-19. https://apps.who.int/iris/bitstream/handle/10665/349321/WHO-2019-nCoV-clinical-2021.2-eng.pdf.

STAR★METHODS

KEY RESOURCES TABLE

REAGENT or RESOURCE	SOURCE	IDENTIFIER
Antibodies		
Anti-Human IgG HRP	Thermofisher	A18805; RRID: AB_2535582
Anti-Human IgG1 HRP	Thermofisher	A55739; RRID: AB_2925764
Anti-Human IgG3 HRP	Thermofisher	SA5-10204; RRID: AB_2665317
Anti-Human IgG HRP	Biorad	172-1033l; RRID: AB_11125145
mouse anti-human placental alkaline phosphatase	Abcam	ab212383/ALP870
anti-human FcRn	Abcam	ab193148; RRID: AB-2801386
mouset anti-human CD16	Cell Signaling	88251S
goat anti-mouse IgG2a	Invitrogen	A-21133; RRID: AB-2535772
goat anti-mouse IgG2b	Invitrogen	A-21141; RRID: AB-2535778
goat anti-rabbit IgG	Invitrogen	A-21070; RRID: AB_2535731
Dapi	Thermofisher	D1360
Bacterial and virus strains		
HSV-1(B^3x1.1)	Montefiore	
Chemicals, peptides, and recombinant proteins		
HSV-1 gD protein	Albert Einstein College of Medicine Protein Core	
HSV-1 gB protein	Albert Einstein College of Medicine Protein Core	
0.1M Glycine	Thermofisher	21004
1M Tris-HCl (pH-8)	Thermofisher	15568025
PNGaseF	N-zyme scientific	NZPP010
Background Sniper	Biocare Medical	BS966
Vector true	Vector Laboratories	SP8400-15
Vectashield mounting media	Vector Laboratories	H-1000
Protein A Columns	Thermofisher	20356
Protein L Columns	Thermofisher	89963
30000 KD molecular weight protein concentrator	Thermofisher	88522
PGC Spin Columns	Thermofisher	60106407
Iodomethane	Sigma	289566
Anhydrous dimethylsulfoxide	Sigma	276855
Spin Columns	Harvard Apparatus	744401
Hydroxide beads	Sigma	367176
DHB Matrix	Sigma	63543
Critical commercial assays		
IgG (Total) Human ELISA Kit	Invitrogen	BMS2091
IgG1 Human ELISA kit	Invitrogen	BMS2092
IgG3 Human ELISA kit	Invitrogen	BMS2094
SARS-CoV-2 IgM	Millipore Sigma	HC19SERM1-85K
SARS-CoV-2 IgA	Millipore Sigma	HC19SERA1-85K
SARS-CoV-2 IgG	Millipore Sigma	HC19SERG1-85K
ADCC FcgRIIIa (human) Reporter Bioassay	Promega	G7015
FcγRI-activating (human) Reporter Bioassay	Promega	GA1341

(*Continued on next page*)

Continued

REAGENT or RESOURCE	SOURCE	IDENTIFIER
FcγRIIa-activating (human) Reporter Bioassay	Promega	G9901
Lumit FcRn Binding Immunoassay	Promega	W1151
Experimental models: Cell lines		
Vero	Albert Einstein College of Medicine	
Software and algorithms		
GraphPad Prism Version 9.1.2	GraphPad Software	
STATA Software Version 15.1	STATA	

RESOURCE AVAILABILITY

Lead contact

Subsequent inquiries and requests for materials and chemicals should be sent to and will be fulfilled by the lead contact, Betsy Herold, M.D. (betsy.herold@einsteinmed.edu).

Materials availability

This study did not generate new unique reagents.

Data and code availability

- All data reported in this paper will be shared by the lead contact upon request.
- This paper does not report original code.
- Any additional information required to reanalyze the data reported in this paper is available from the lead contact upon request.

EXPERIMENTAL MODEL AND STUDY PARTICIPANT DETAILS

Pregnant women receiving care at Montefiore Medical Center, Bronx, NY were recruited for participation and provided written informed consent; the study was approved by the Albert Einstein College of Medicine Institutional Review Board (IRB # 086757). The pre-COVID enrollment was conducted between October 2018 and December 2019 and the SARS-CoV-2 maternally-coinfected dyads were recruited between April and December 2020. SARS-CoV-2 testing of nasopharyngeal secretions was conducted by the Clinical Microbiology Lab. Pregnant women were excluded for HIV infection and anemia (Hgb < 10 g/dL). Blood was collected from mothers during a routine clinical blood draw either during the third trimester or at presentation in labor; cord blood was collected at delivery. Plasma was isolated from cells within 24 hours of sample collection, divided into aliquots, and stored at -80°C. Maternal blood was tested for HSV-1 and HSV-2 IgG by HerpeSelect 1 and 2 Immunoblot IgG (cat # IB0900G, Focus Diagnostics, Cypress, CA) and participants were excluded from further study if they were both HSV-1 and HSV-2 seronegative. Clinical data extracted from the medical record included age, demographics including race and ethnicity, mode of delivery, diagnosis of preeclampsia or chorioamnionitis and, for SARS-CoV-2+ participants, disease severity as classified by the World Health Organization guidelines.[46] Patient demographics information is included in Table 1.

METHOD DETAILS

IgG responses

Total IgG, IgG1 and IgG3 were quantified using a commercial ELISA kits (IgG (Total) Human ELISA kit (cat #: BMS2091, Invitrogen, Carlsbad, CA), IgG1 Human ELISA kit (cat #: BMS2092, Invitrogen) and IgG3 Human ELISA kit (cat #: BMS2094, Invitrogen). HSV-specific IgG, IgG1, IgG3 were quantified by ELISA using specific-secondary antibodies. ELISA plates were coated overnight with HSV-1(B^3x1.1) infected Vero cell lysate at a multiplicity of infection of 0.1 plaque-forming unit per cell or uninfected Vero cell lysates.[39] Wells were then blocked with 5% bovine serum albumin and then incubated with serial plasma dilutions of the samples overnight in duplicate wells. Bound human IgG, IgG1 and IgG3 was quantified using specific horseradish peroxidase (HRP)- conjugated secondary antibodies (Thermofisher). The dilution that yielded a 50% reduction in maximal optical densitometry units (odu) after subtracting odu obtained for uninfected Vero cell lysates as illustrated in Figure S3 was determined for the study population and results reported as odu at that dilution (1:12,500 for anti-HSV IgG, 1:2500 for IgG1 and IgG3). To detect gD and gB specific antibodies, plates were coated with 10 μg of recombinant gD-1 or gB-1 protein[29] and then incubated with serial dilutions of plasma and secondary antibodies as for infected cell lysates.[31] Transfer ratios (TR) were calculated as the ratio of cord to maternal odu at the indicated dilution. SARS-CoV-2 IgM, IgA and IgG against spike proteins were determined using a Luminex bead assay (cat #: HC19SERG1-85K for IgG, HC19SERM1-85K for IgM and HC19SERA1-85K for IgA, Millipore Sigma, Burlington, MA).

Functional antibody assays

Neutralization of HSV-1(B3x1.1), a clinical isolate, was assessed by plaque reduction assay. Serial 2-fold heat-inactivated plasma dilutions were incubated with HSV-1(B3x1.1) (75-100 plaque-forming units) for 1 hour before inoculating Vero cells. Plaques were counted after 48 hours, and the neutralization titer was defined as the plasma dilution that yielded a 50% reduction in viral plaque numbers relative to cells treated with virus only control (Figure S3).[39] C1q binding antibodies were quantified by ELISA. Plates were coated with HSV-1(B3x1.1) infected Vero cell lysate or uninfected lysate overnight.[39] Plates were blocked and then incubated with serial dilutions of heat-inactivated plasma samples followed by 2-hour incubation with 1μg/ml of human C1q complement (Complement Technology), and bound C1q was then quantified with 1μg/ml of anti-human C1q-HRP conjugated antibody (Complement Technology). The dilution that yielded a 50% reduction in odu after subtracting the odu for uninfected cell lysate (1:20) was used to report the data. FcγRIIIa activation, a biomarker for ADCC, was assayed using the ADCC FcγRIIIa (human) Reporter Bioassay (cat #: G7015, Promega, Madison, WI) with 1:5 dilution of plasma. Fold-induction was calculated relative to luciferase activity in the absence of plasma after subtracting the background for uninfected cells. Similar bioassays were conducted to measure FcγRI- and FcγRIIa-activating HSV IgG (cat # GA1341 and G9901: Promega, Madison, WI). The relative of affinity of IgG for the FcRn was measured using the Lumit FcRn Binding Immunoassay (Cat #: W1151, Promega). Human IgG1 labeled with large BiT (Tracer-LgBiT) was used as the tracer and was incubated with C-terminal biotinylated human FcRn bound to Streptavidin-SmBiT (hFcRn-Biotin-SA-SmBiT), which yields a maximal luminescence signal (SpectraMax M5, Molecular Devices, CA). Test samples were added (in duplicate) and the decrease in luminescent signal reflecting competition with the Tracer-LgBit for binding to the FcRn was determined. Results are presented as 1/relative K_D.

Enrichment for anti-gD, gB, IgG1 or IgG3 antibodies

Individual or pooled plasma samples (2 ml/sample) were applied to a Protein L column (cat # 89963, Thermofisher, Waltham, MA) per manufacture's guidelines, incubated for 1h at room temperature, washed 3 times with 2 ml of phosphate buffered saline (PBS, pH7.0) and Ig eluted from the column with 0.1M glycine in 1 ml (pH 2-3) (cat # 21004, Thermofisher). The flow through and eluent were neutralized with 1M Tris-HCl (pH 8) (cat # 15568025, Thermofisher). The buffer was exchanged with PBS and samples concentrated using a 30,000 KD molecular weight Protein Concentrator (cat # 88522, Thermo Fisher) and resuspended in 1 ml total volume. The Ig-enriched samples were then either incubated with lectin-gD or lectin-gB agarose column for 1 hour, bound Ig eluted with 0.1M glycine, neutralized to pH 7 with 1M Tris-HCl, buffer exchanged and concentrated as above. Alternatively, the Protein L eluent was applied to a Protein A column (cat # 20356, Thermofisher), which binds human IgG1, IgG2 and IgG4 but not IgG3. A subset of samples was sequentially incubated with a gD or gB lectin agarose column followed by a Protein A column to enrich for IgG1 or IgG3 specific anti-gD and gB. After concentration, the total protein was quantified by nanodrop and all samples were diluted to a final concentration of 0.5 mg/ml for functional assays.

Western blots

Western blots were prepared with 5 μg of recombinant gD-1 or gB-1 protein produced in HEK293 cells [29]or 10 μg HSV-1-infected or uninfected Vero cell lysates per lane, proteins separated by SDS-PAGE, transferred to nitrocellulose and immunoblotted with10 μg/ml of enriched IgG samples in blocking buffer overnight followed by anti-human IgG-HRP (1:500) (cat #: 1721033, BioRad, Hercules, CA). Blots were scanned using ChemiDoc imaging system equipped with GelDOC2000 software.

Glycan analysis

The IgG enriched for anti-gB and anti-gD antibodies underwent deglycosylation by incubating overnight with PNGaseF (cat #: NS99010, N-zyme scientific, Doylestown, PA) in PBS at 37°C. The deglycosylated IgG samples were then precipitated using cold ethanol, and the supernatant containing the released native N-glycans was collected and dried using vacuum centrifugation. To desalt the samples, they were resuspended in 0.1% trifluoroacetic acid and loaded onto graphite spin columns containing porous graphitized carbon (PGC) (cat #: 60106407, Thermofisher). The native N-glycans were washed with 0.1% trifluoroacetic acid and eluted from the graphite spin column using 25% acetonitrile/0.1% trifluoroacetic acid. Subsequently, the eluted N-glycans were dried using vacuum centrifugation. Permethylation of the native N-glycans was performed by combining the samples with iodomethane (cat #: 289566, Sigma-Aldrich, St. Louis, MO) in anhydrous dimethyl sulfoxide (cat #: 276855, Sigma-Aldrich). The mixture was then loaded onto spin columns containing sodium hydroxide beads (cat #: 367176, Sigma-Aldrich). Purification of the resulting permethylated N-glycans was achieved through liquid-liquid extraction using a 1:1 chloroform/methanol mixture. The chloroform layer, which contained the permethylated N-glycans, was collected and dried under nitrogen gas. The dried permethylated N-glycans were re-suspended in 50% methanol. A 1 μl sample was mixed with super-DHB matrix (cat #: 63542, Sigma-Aldrich) at a 1:1 ratio and spotted onto an MTP 384 well-polished steel target plate (Bruker Daltonics, Billerica, MA). Analysis of the samples was performed using MALDI-TOF with the Ultraflextreme mass spectrometer (Bruker Daltonics). The acquisition software used was FlexControl 3.4, and the raw data was processed using FlexAnalysis 4.0 software. The resulting mass spectra were converted to peak lists. To determine the percent composition of each N-glycan, the raw abundance of each N-glycan was divided by the sum of the abundances of all N-glycans.

Immunohistochemistry of placental tissue

Paraffin embedded placental tissue sections were obtained from the Pathology Laboratory from a subset of the enrolled SARS-CoV-2 positive and contemporaneous SARS-CoV-2 PCR negative deliveries (Placental tissue from the pre-COVID cohort was not available). The tissue was deparafinized in xylene and rehydrated in an alcohol series. Samples were then boiled for in 10 mM sodium citrate (pH 6.0) for 30 min, blocked with Background Sniper (cat#: BS966, Biocare Medical, Pacheco, CA) for 15 min. The tissues were then incubated with primary antibodies (mouse anti-human placental alkaline phosphatase 1:1000 (cat#: ab212383, Abcam, Cambridge, UK); anti-human FcRn 1:100 (cat#: ab193148, Abcam) and rabbit anti-human CD16 1:100 (cat#: NCL-L-CD16, Leica Biosystems, Wetzlar, Germany) in 5% bovine serum albumin (BSA) in PBS overnight at 4°C. Slides were washed in 0.1% PBS-Tween and incubated for 2h with the fluorescently-conjugated secondary antibodies (goat anti-mouse IgG2a (cat # A-21133, Abcam); goat anti-mouse IgG2b (cat # A-21141, Abcam); or goat anti-rabbit (cat # A-21070, Thermofisher). At a dilution of 1:500 in 5% BSA. Finally, slides were treated with Vector true (cat # SP8400-15, Vector Laboratories, Newark, CA), nuclei stained with DAPI (cat # D1360, Thermofisher) and cover slips applied with Vectashield mounting media (cat # H-1000, Vector Laboratories). Images were acquired with an SP8 Lightning confocal microscope and intensity calculated using Image J software.

QUANTIFICATION AND STATISTICAL ANALYSIS

Unpaired t-test, Wilcoxon matched signed rank paired, Mann-Whitney, Chi-square and ANOVA with Tukey's multiple comparison test or Kruskal Wallis with Dunn's multiple comparison were determined using GraphPad Prism, version 9.1.2 software (GraphPad Software Inc. San Diego, CA). A P-value of 0.05 was considered statistically significant. Linear and multivariable linear regression models were built using STATA Software, version 15.1 to identify factors associated with transfer of HSV-specific IgG, nAbs or FcγRIIIa activating IgG.